ЖЭТФ, 2006, том 129, вып. 4, стр. 751–760

INFRARED ABSORPTION AND RAMAN SCATTERING ON COUPLED PLASMON–PHONON MODES IN SUPERLATTICES

L. A. Falkovsky [a*], ***E. G. Mishchenko*** [a,b]

[a] *Landau Institute for Theoretical Physics*
119337, Moscow, Russia

[b] *Department of Physics, University of Utah*
Salt Lake City, UT 84112

Received November 7, 2005

We theoretically consider a superlattice formed by thin conducting layers spatially separated between insulating layers. The dispersion of two coupled phonon–plasmon modes of the system is analyzed by using the Maxwell equations, with the retardation effect included. Both transmission for the finite plate and the absorption for the semi-infinite superlattice in the infrared are calculated. Reflectance minima are determined by the longitudinal and transverse phonon frequencies in the insulating layers and by the density-state singularities of the coupled modes. We also evaluate the Raman cross section from the semi-infinite superlattice.

PACS: 63.22.+m, 73.21.Cd, 78.30.-j

1. INTRODUCTION

Coupling of collective electron oscillations (plasmons) to optical phonons in polar semiconductors was predicted more than four decades ago [1], experimentally observed using Raman spectroscopy in n-doped GaAs [2], and extensively investigated since then (see, e.g., [3]). On the contrary, the interaction of optical phonons with plasmons in semiconductor superlattices is much less studied. A two-dimensional electron gas (2DEG) created at the interface of two semiconductors has the properties that differ drastically from the properties of its three-dimensional counterpart. In particular, the plasmon spectrum of the 2DEG is gapless [4] owing to the long-range nature of the Coulomb interaction of carriers, $\omega^2(k) = v_F^2\kappa_0 k/2$, where v_F is the Fermi velocity and κ_0 is the inverse static screening length in the 2DEG. Coupling of 2D plasmons to optical phonons has been considered in Refs. [5, 6] for a single 2DEG layer. The resulting coupling is usually nonresonant because the characteristic phonon energies (30–50 meV) are several times larger than typical plasmon energies. Still, hybrid plasmon–optical-phonon modes are of considerable interest in relation to polaronic transport phenomena [7], Raman spectroscopy, and infrared optical absorption experiments.

Plasmon excitations in a periodic system of the electron layers have been discussed in a number of theoretical papers [8, 9], disregarding the phonon modes. In the present paper, we analyze the coupled phonon–plasmon modes for a superlattice of 2D electron layers placed between insulating layers and demonstrate the possibility of a stronger resonant coupling of plasmons to optical phonons excited in the insulator. This enhancement occurs in superlattices due to the interaction of plasmons in different layers that spreads the plasmon spectrum into a mini-band spanning the energies from zero up to the new characteristic energy $v_F\sqrt{\kappa_0/d}$, where d is the interlayer distance [10]. This value could exceed typical phonon frequencies leading to formation of resonant hybrid modes around crossings of phonons and band plasmons.

The coupled phonon–plasmon modes are usually considered in the so-called electrostatic approximation, with the retardation effect ignored and the terms of ω/c in the Maxwell equations neglected in comparison with the terms having values of the wave vector k. This is correct if the Raman scattering is studied, when ω has the meaning of the frequency transfer. Then, ω is much less than the incident frequency $\omega^i \sim ck$. But if we are

*E-mail: falk@itp.ac.ru

interested in absorption for the infrared region, where ω is the frequency of incident light and corresponds to the optical phonon frequency, ω and ck are comparable. In this case, the retardation effect must be fully included.

The plan of this paper (preliminary results were published in Ref. [11]) is as follows. In Sec. 2, the Maxwell equations for the periodic system of thin conducting layers sandwiched between the insulating layers are solved, yielding the spectrum of coupled phonon–plasmon modes. In Sec. 3, we consider absorption of a finite sample of layers and reflectance of a semi-infinite system in the infrared region. In Sec. 4, we analyze the Raman light scattering from a semi-infinite system of layers.

2. SPECTRUM OF COUPLED MODES

We consider a superlattice formed by periodically grown layers of two polar semiconductors (e.g., GaAs and AlGaAs) with 2DEG layers formed in the interface regions (Fig. 1).

For simplicity, we assume a superlattice with a single period d and the thickness of a 2DEG layer much less than the period. We also neglect the difference in bulk phonon properties of the two materials. Optical phonons in polar semiconductors are most conveniently described within the dielectric continuum model, which yields the familiar phonon contribution to the dielectric function,

$$\varepsilon = \varepsilon_\infty \frac{\omega_{LO}^2 - \omega^2 - i\omega\Gamma}{\omega_{TO}^2 - \omega^2 - i\omega\Gamma},$$

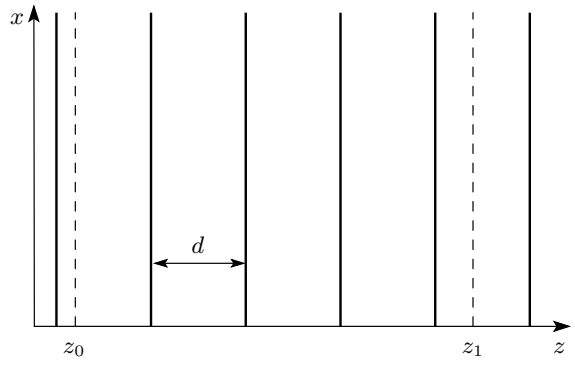

Fig. 1. The stack of conducting 2D layers sandwiched between dielectric layers of thickness d with the dielectric constant $\varepsilon(\omega)$; z_0 and z_1 are the boundaries (dashed lines) of the sample if a finite stack is considered

where ω_{LO} and ω_{TO} are the frequencies of longitudinal and transverse optical phonons respectively, and Γ is the the phonon width (we do not distinguish the widths of the TO and LO modes).

Collective modes of our system are described by the Maxwell equations, which in the Fourier representation with respect to time have the form

$$\nabla(\nabla\cdot\mathbf{E}) - \nabla^2\mathbf{E} = \varepsilon\frac{\omega^2}{c^2}\mathbf{E} + \frac{4\pi i\omega}{c^2}\mathbf{j}, \qquad (1)$$

where the last term involves the in-plane electric currents $\mathbf{j}$ induced in the 2DEG layers by the electric field $\mathbf{E}$. As usual, when the frequency of the collective mode lies above the electron–hole continuum, it is sufficient to use the Drude conductivity to describe the in-plane electric currents,

$$\mathbf{j}_\parallel(\omega,x,z) = \frac{ie^2 n_e}{m(\omega+i\gamma)}\sum_n \delta(z-z_n)\mathbf{E}_\parallel(\omega,x,z), \qquad (2)$$

where $z_n = nd$ are positions of interfaces (n is an integer corresponding to the periodicity of the stack), $n_e = p_F^2/2\pi\hbar^2$ and m are the electron density (per the surface unit) and the effective mass, γ is the electron collision frequency, and x and z are the coordinates along and perpendicular to the interfaces, respectively.

We consider the case of p-polarization, where the field $\mathbf{E}$ lies in the xz plane and therefore the current $\mathbf{j}$ has then only the x-component. Using the Fourier transformations with respect to the x coordinate, $\mathbf{E} \propto \exp(ik_x x)$, we can rewrite Maxwell equations (1) as

$$ik_x\frac{dE_z}{dz} - \frac{d^2E_x}{dz^2} - \varepsilon\frac{\omega^2}{c^2}E_x = \frac{4\pi i\omega}{c^2}j_x,$$

$$ik_x\frac{dE_x}{dz} + \left(k_x^2 - \varepsilon\frac{\omega^2}{c^2}\right)E_z = 0.$$

Eliminating

$$E_z = -\frac{ik_x}{\kappa^2}\frac{dE_x}{dz},$$

we obtain the equation for E_x,

$$\left(\frac{d^2}{dz^2} - \kappa^2 + 2\kappa C\sum_n \delta(z-z_n)\right)E_x(\omega,k_x,z) = 0, \qquad (3)$$

where

$$C = \frac{2\pi n_e e^2\kappa}{\varepsilon\omega(\omega+i\gamma)m}, \quad \kappa = \sqrt{k_x^2 - \varepsilon\frac{\omega^2}{c^2}}.$$

At the interfaces $z = z_n$, the E_x-component must be

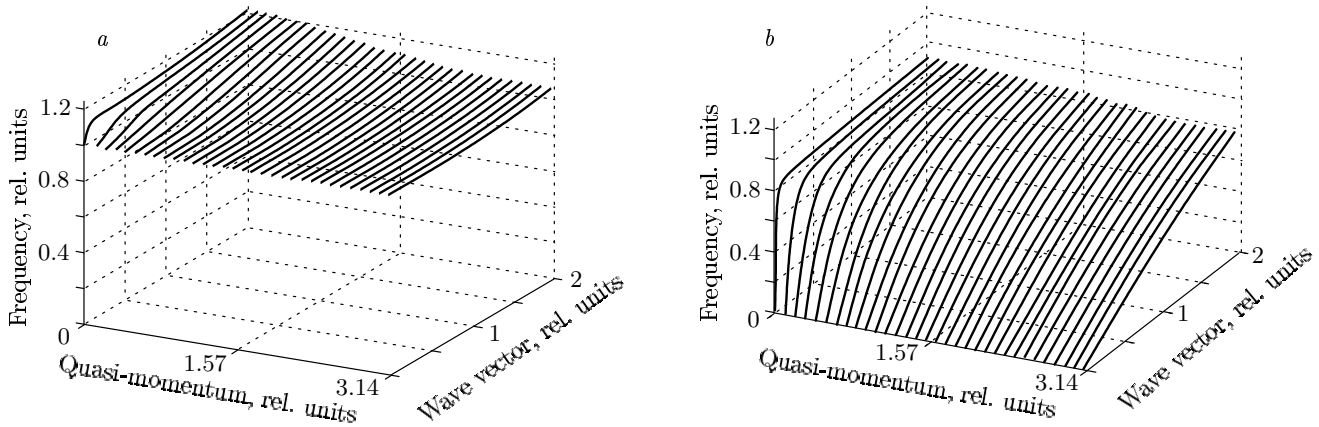

Fig. 2. The phonon-like (a) and plasmon-like (b) modes $\omega_\pm(k_x, k_z)$ (their character is defined at small wave vectors k_x) of an infinite number of 2D metallic layers (with the carrier concentration in every layer $n_e = 3 \cdot 10^{11}$ cm^{-2}) sandwiched between dielectric layers of thickness d. The frequencies $\omega_\pm(k_x, k_z)$ in units of the phonon frequency ω_{LO} are plotted as functions of the in-plane wave vector k_x and the quasi-momentum $k_z < \pi/d$ (both in units $1/d$). The parameters used here are reported in the literature for GaAs: $\omega_{LO} = 36.5$ meV, $\omega_{TO} = 33.6$ meV, $\varepsilon_\infty = 10.6$; the thickness is taken as $d = 1/\kappa_0$, the screening length $\kappa_0 = 2me^2/\hbar^2\varepsilon_\infty = 2.5 \cdot 10^6$ cm^{-1}

continuous and the z-component of the electric induction εE_z has a jump,

$$\varepsilon(E_z|_{z=nd+0} - E_z|_{z=nd-0}) = \\ = 4\pi \int\limits_{nd-0}^{nd+0} \rho(\omega, k_x, z)\, dz, \quad (4)$$

where the carrier density is connected to current (2) by the continuity equation

$$\rho(\omega, k_x, z) = j_x(\omega, k_x, z) k_x/\omega. \quad (5)$$

For the infinite stack of layers, $-\infty < n < \infty$, independent solutions of Eqs. (3) and (4) represent two Bloch states $E_x(z) = f_\pm(z)$ moving along positive and negative directions of the z axis,

$$f_\pm(z) = \exp(\pm ik_z nd)\left\{\mathrm{sh}\left[\kappa(z-nd)\right] - \exp(\mp ik_z d) \times \right.$$

$$\left. \times\, \mathrm{sh}\left[\kappa(z-(n+1)\,d)\right]\right\}, \quad nd < z < (n+1)\,d, \quad (6)$$

with the quasi-momentum k_z determined from the dispersion equation

$$\cos(k_z d) = \mathrm{ch}(\kappa d) - C\,\mathrm{sh}(\kappa d). \quad (7)$$

The quasi-momentum k_z can be restricted to the Brillouin half-zone $0 < k_z < \pi/d$ if the phonon and electron damping vanishes. In the general case, we fix the choice of the eigenfunctions in Eq. (6) by the condition $\mathrm{Im}\, k_z > 0$, such that the solution f_+ decreases in the positive direction z. Equation (7) implicitly determines the spectrum $\omega_\pm(k_x, k_z)$ of two coupled plasmon–optical-phonon modes shown in Fig. 2 as functions of the in-plane wave vector k_x and the quasi-momentum k_z. These modes are undamped if the electron collision rate and the phonon width are small. The modes arise from the interaction of the plasmon branch in the 2DEG and the phonon LO mode in the 3D insulator. They have a definite character far from the intersection of the corresponding dispersion curves. For instance, at small values of k_x, the $\omega_+(k_x, k_z)$ mode is mainly the phonon mode, whereas the $\omega_-(k_x, k_z)$ mode has mainly the plasmon character. At large values of k_x, they interchange their character.

We note that $k_x = k_z = 0$ is a saddle point for both branches $\omega_\pm(k_x, k_z)$. In the vicinity of this point, the frequency grows as a function of k_x and decreases with increasing k_z. This is evident from Fig. 3 and can be explicitly shown in the limit of $k_x \gg \omega|\varepsilon(\omega)|/c$, when the retardation effects of the electromagnetic field are negligible. Then, $\kappa \approx k_x$ and Eq. (7) yields two solutions,

$$\omega_\pm^2(k_x, k_z) = \frac{1}{2}(\Omega^2 + \omega_{LO}^2) \pm \\ \pm \frac{1}{2}\left[(\Omega^2 + \omega_{LO}^2)^2 - 4\Omega^2\omega_{TO}^2\right]^{1/2}, \quad (8)$$

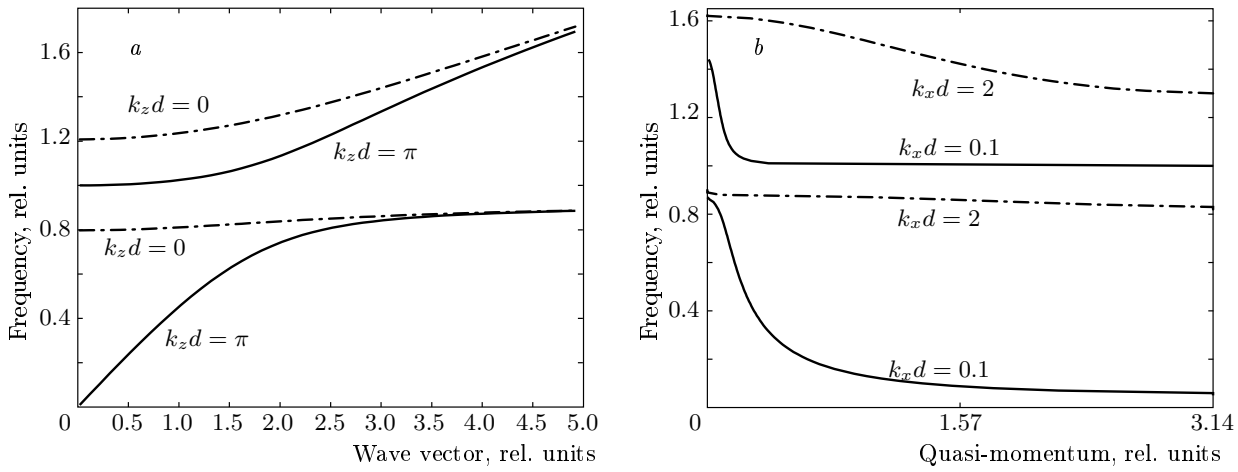

Fig. 3. Dispersion of coupled phonon–plasmon modes of an infinite number of 2D metallic layers sandwiched between dielectric layers. The frequencies $\omega_\pm(k_x, k_z)$ (in units of ω_{LO}) are plotted as functions of (a) the in-plane wave vector k_x for two values of the quasi-momentum k_z and (b) the quasi-momentum k_z for two values of the in-plane wave vector k_x; $k_{x,z}$ in units of the inverse period $1/d = 2.5 \cdot 10^6$ cm^{-1}. The dash-dotted lines represent the upper boundary $\omega_\pm(k_x, k_z = 0)$ of two phonon–plasmon modes and the solid lines mark the lower boundary corresponding to $\omega_\pm(k_x, k_z = \pi/d)$. The parameters are the same as in Fig. 2

where we introduced the notation

$$\Omega^2(k_x, k_z) = \omega_0^2(k_x)\frac{\mathrm{sh}(k_x d)}{\mathrm{ch}(k_x d) - \cos(k_z d)},$$

$$\omega_0^2(k_x) = \frac{2\pi n_e e^2 k_x}{m\varepsilon_\infty}$$

and omitted the phonon and electron damping. The frequency $\omega_0(k_x)$ is the conventional square-root spectrum of 2D plasmons in the limit of layer separation large compared to the wavelength, $d \gg k_x^{-1}$. The quantity $\Omega(k_x, k_z)$ describes the plasmon spectrum that would exist in a superlattice consisting of nonpolar semiconductors (when $\omega_{LO} = \omega_{TO}$).

The mode $\omega_+(k_x, k_z)$ has a gap, while the other mode has a linear dispersion, $\omega_-(k_x, k_z) = s(k_z)|k_x|$ at $k_x \ll d^{-1}, k_z$, with the velocity given by

$$s(k_z) = v_F\sqrt{\frac{\kappa_0 d}{2[1 - \cos(k_z d)]}},$$

where $\kappa_0 = 2me^2/\hbar^2\varepsilon_\infty$ is the static screening radius in the 2DEG. For a fixed value of the in-plane wave vector k_x, every mode develops a band (with respect to the quasi-momentum k_z) with boundaries, $\omega_{upper}(k_x) \le \omega(k_x, k_z) \le \omega_{lower}(k_x)$, where

$$\omega_{upper}^2 = \Omega^2(k_x, 0) = \omega_0^2(k_x)\,\mathrm{cth}\,\frac{k_x d}{2}$$

for the upper boundary and

$$\omega_{lower}^2 = \Omega^2\left(k_x, \frac{\pi}{d}\right) = \omega_0^2(k_x)\,\mathrm{th}\,\frac{k_x d}{2}$$

for the lower boundary. Figure 3b illustrates the behavior of the gapless, so-called acoustic mode for small values of $k_z < k_x$, where it acquires a gap. We see that the frequency of this mode decreases rapidly in the region $k_z > k_x$.

In the rest of the paper, we analyze various experimental implications resulting from the existence of hybrid plasmon–phonon modes. Such modes can be observed in both the infrared absorption and Raman spectroscopy.

3. INFRARED ABSORPTION ON COUPLED PLASMON–PHONON MODES

We now calculate the reflectance and the transmission of a plane wave with the p-polarization, incident from the vacuum on a thin plate consisting of a stack of layers. We suppose that the boundaries of the sample are parallel to the layers and intersect the z axis at z_0 and $z_1 = Nd + \tilde{z}_1$ with $0 < z_0$, $\tilde{z}_1 < d$ (see Fig. 1). We assume that

$$E_x(z) = \exp\left[ik_z^i(z - z_0)\right] + A\exp\left[-ik_z^i(z - z_0)\right]$$

in the vacuum ($z < z_0$), where $k_z^i = \sqrt{(\omega/c)^2 - k_x^2}$ and A is the amplitude of the reflected wave. In the region $z > z_1$, the transmitted wave has the form

$$E_x(z) = T\exp[ik_z^i(z - z_1)],$$

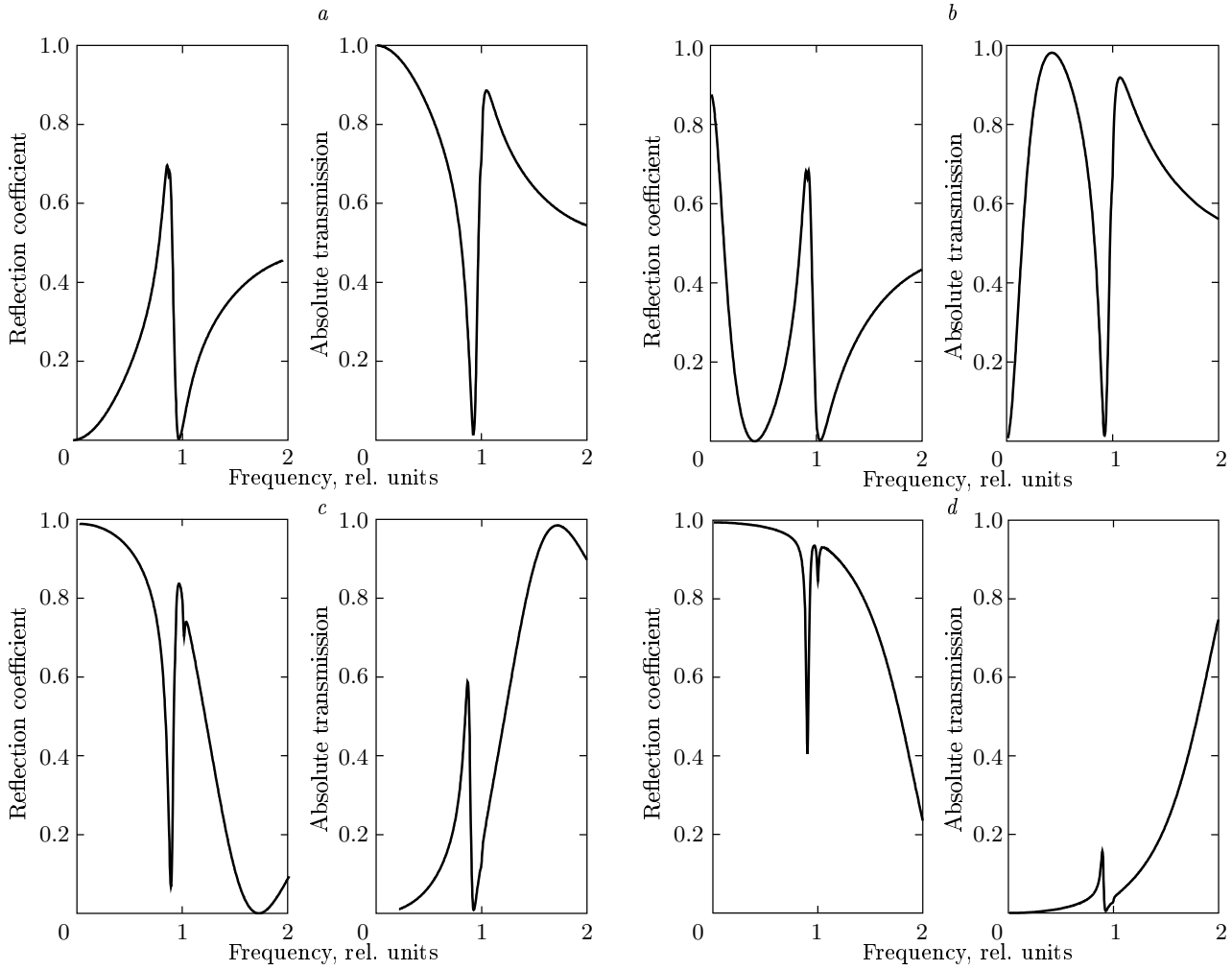

Fig. 4. Calculated p-polarized reflection–absorption spectra of GaAs plates (of the thickness $l = 300d$) with the superlattices of different electron concentrations in a layer: a — $n_e = 0$; b — $n_e = 5 \cdot 10^{10}$ cm^{-2}; c — $n_e = 6 \cdot 10^{11}$ cm^{-2}; d — $n_e = 1.2 \cdot 10^{12}$ cm^{-2}. The frequencies, the phonon width $\Gamma = 0.01$, and the electron relaxation frequency $\gamma = 0.01$ are given in units of ω_{LO}. The incidence angle is $\theta = \pi/4$. Other parameters are the same as in Fig. 2

and we seek the field inside the plate as a sum of two solutions (6),

$$E_x(z) = C_+ f_+(z) + C_- f_-(z),$$

with the definite values of k_x, ω, and $k_z = k_z(\omega, \kappa)$ obeying dispersion equation (7).

As usual, the boundary conditions at z_0 and z_1 require the continuity of the x-component E_x of the electric field parallel to the layers and of the z-component D_z of the electric induction normal to the layers. The second condition rewritten via the electric field E_x gives, e.g., at $z = z_0$,

$$\frac{\varepsilon}{\kappa^2} E'_x(z_0+) = -\frac{1}{k_z^{i2}} E'_x(z_0-).$$

The boundary conditions give the following equations for C_+, C_-, A, and T:

$$\begin{aligned} 1 + A &= C_+ f_+(z_0) + C_- f_-(z_0), \\ -1 + A &= \left[C_+ f'_+(z_0) + C_- f'_-(z_0)\right] \varepsilon k_z^i / i\kappa^2, \\ T &= C_+ f_+(z_1) + C_- f_-(z_1), \\ -T &= \left[C_+ f'_+(z_1) + C_- f'_-(z_1)\right] \varepsilon k_z^i / i\kappa^2. \end{aligned}$$

Solving these equations, we find the transmitted amplitude

$$T = \frac{2\varepsilon k_z^i}{i\kappa^2} \frac{f'_+(z_1) f_-(z_1) - f_+(z_1) f'_-(z_1)}{a_{11} a_{22} - a_{12} a_{21}}$$

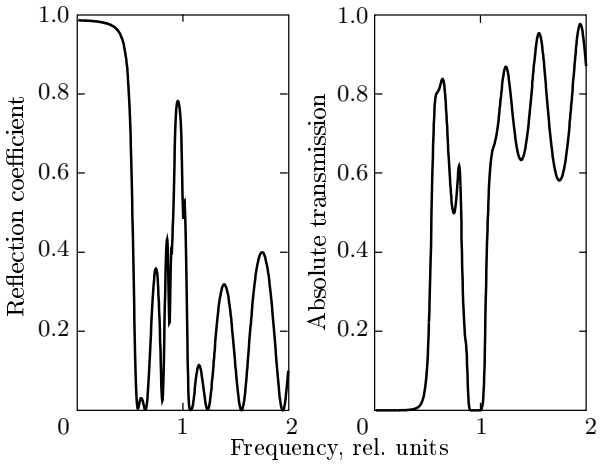

Fig. 5. Interference in the sample of thickness $l = 3000d$, $d = 4 \cdot 10^{-7}$ cm; the electron concentration is 10^{11} cm^{-2}

and the reflected amplitude

$$A = -1 + 2\frac{a_{21}f_-(z_0) - a_{22}f_+(z_0)}{a_{11}a_{22} - a_{12}a_{21}},$$

where

$$a_{11} = f'_+(z_0)\varepsilon k_z^i/i\kappa^2 - f_+(z_0),$$

$$a_{22} = f'_-(z_1)\varepsilon k_z^i/i\kappa^2 + f_-(z_1),$$

$$a_{12} = f'_-(z_0)\varepsilon k_z^i/i\kappa^2 - f_-(z_0),$$

$$a_{21} = f'_+(z_1)\varepsilon k_z^i/i\kappa^2 + f_+(z_1).$$

The transmission $|T|^2$ and reflection $|A|^2$ coefficients are shown in Fig. 4 for samples with various electron concentrations n_e. The incidence angle is taken $\theta = \pi/4$. Other parameters are as follows: the thickness $l = Nd = 300d$, the lattice period $d = 1/\kappa_0 = 4 \cdot 10^{-7}$ cm, the phonon width $\Gamma = 0.02\omega_{LO}$, and the electron scattering rate $\gamma = 0.01\omega_{LO}$. For all concentrations, $k_z d \ll 1$, and there are many layers on the wave length of the field. Therefore, the reflectance is not sensitive to the sample surface positions z_0 and $\tilde{z}_1$. But if the thickness d is larger, as shown in Fig. 5, an interference phenomenon is seen.

To avoid the interference effect, we have calculated the reflectance for a semi-infinite sample. The results can be seen in Fig. 6, where the theoretical curves are presented for the various electron concentrations and the lattice periods. There is a singularity at ω_{LO}. For $d = 1/\kappa_0$ and the intermediate electron concentration in the layer (the dashed lines in Fig. 6), there are two regions (one is at higher frequencies and the other is just below $\omega_{TO} = 0.9\omega_{LO}$), where the sample with layers is more transparent than the sample without any (shown by the dashed-dotted lines).

This is an effect of the coupled phonon–plasmon modes: the minima of the reflection coefficient correspond to the density-state singularities of the phonon–plasmon coupled modes at $k_z = 0$ and $k_x \to 0$ (see Fig. 3*a*). The frequencies of these singularities are determined by Eq. (8) with $\Omega^2 = 4\pi n_e e^2/md\varepsilon_\infty$. For a large electron concentration (solid lines in Fig. 6), the reflection is incomplete only in the narrow interval bounded by the singularities at ω_{TO} and ω_{LO}. Finally, the reflection coefficient tends to unity at low frequencies because the skin depth of the metallic system goes to infinity in this case. For the sample with the large period $d = 5/\kappa_0$ (Fig. 6*b*), the effect of carriers is seen at a higher concentration.

4. RAMAN SCATTERING FROM COUPLED MODES

We now consider the Raman scattering of the radiation incident from a vacuum with the vector potential $\mathbf{A}^i$, the frequency ω^i, and the wave vector $\mathbf{k}^i$ on the sample occupying the semi-infinite space $z > z_0$, where $0 < z_0 < d$. The corresponding quantities in the scattered wave are denoted by $\mathbf{A}^s$, ω^s, and $\mathbf{k}^s$.

In addition to these fields, an electric field $\mathbf{E}$ is excited in the Raman light scattering in polar crystals along with the longitudinal optical vibrations $\mathbf{u}$. The field $\mathbf{E}$ corresponds to the excitation of plasmons, whereas the vibrations $\mathbf{u}$ are associated with the phonon excitations.

These processes can be described by the effective Hamiltonian

$$\mathcal{H} = \int d^3r\, \mathcal{N}_{jk}(t, \mathbf{r}) A_j^s(t, \mathbf{r}) A_k^i(t, \mathbf{r}), \qquad (9)$$

where the operator

$$\mathcal{N}_{jk}(t, \mathbf{r}) = g_{ijk}^u \hat{u}_i(t, \mathbf{r}) + g_{ijk}^E E_i(t, \mathbf{r}) \qquad (10)$$

is linear in the phonon $\mathbf{u}$ and photon $\mathbf{E}$ operators.

We are interested in the inelastic scattering on the phonon–plasmon coupled modes. Therefore, we assume that the frequency transfer $\omega = \omega^i - \omega^s$ is of the order of the phonon frequencies ω_{LO}, but the frequencies ω^i and ω^s of the incident and scattered fields are much greater than the phonon frequencies. We can then ignore the effect of carriers in the layers on the propagation of both scattered $\mathbf{A}^s(t, \mathbf{r})$ as well as incident

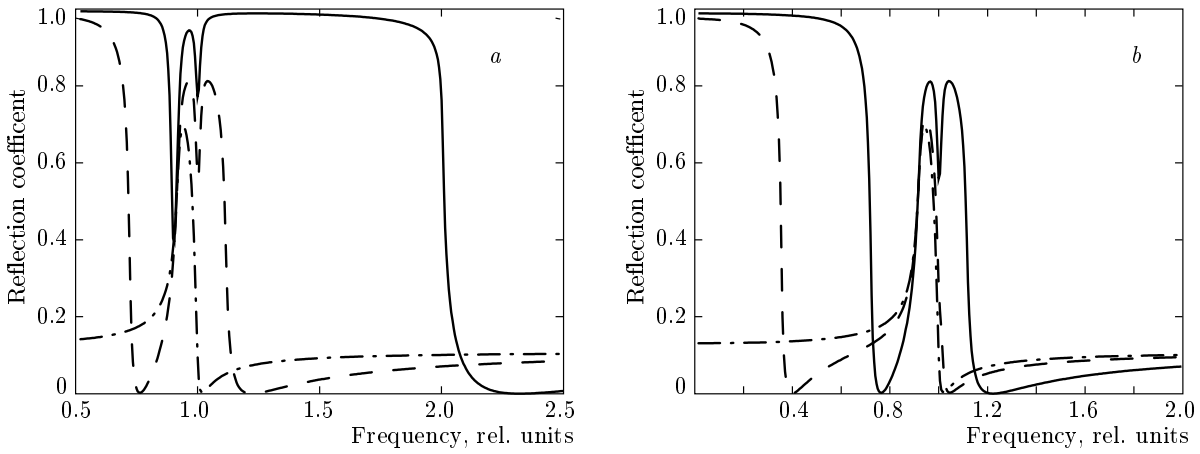

Fig. 6. Calculated p-polarized reflection–absorption spectra for the semi-infinite superlattice versus the frequency in units of ω_{LO} at the incidence angle $\theta = \pi/4$ for different electron concentrations: $n_e = 0$ (dash-dotted lines); $n_e = 2 \cdot 10^{11}$ cm^{-2} (dashed lines), and $n_e = 10^{12}$ cm^{-2} (solid lines); the lattice period is $d = 1/\kappa_0 = 4 \cdot 10^{-7}$ cm (a) and $d = 5/\kappa_0$ (b); the phonon width is $\Gamma = 0.01$ and the electron relaxation rate is $\gamma = 0.01$ (in units ω_{LO})

$\mathbf{A}^i(t, \mathbf{r})$ light, taking the incident field in the sample ($z > z_0$) in the form

$$t_j \exp[ik_z^i(z - z_0)],$$

normalized to the incident flow; t_j is the transmission coefficient from the vacuum to the sample, $k_z^i = \sqrt{\varepsilon(\omega^i)(\omega^i/c)^2 - k_x^{i2}}$.

When the scattered field $\mathbf{A}^s$ is taken as a variable in Hamiltonian (9), we obtain an additional current $\mathbf{j}^s(t, \mathbf{r})$,

$$-c\frac{\delta \mathcal{H}}{\delta A_j^s} = j_j^s(t, \mathbf{r}) = -c\mathcal{N}_{jk}(t, \mathbf{r})A_k^i(t, \mathbf{r}), \qquad (11)$$

in the Maxwell equation for this field. The phonon and plasmon fields in the operator $\mathcal{N}_{jk}(t, \mathbf{r})$ are the source of the Raman scattering, whereas the incident field $\mathbf{A}^i(t, \mathbf{r})$ is considered as an external force for scattering.

Eliminating the z-component, we write the Maxwell equation for the p-polarization of the scattered field (xz is the scattering plane) as

$$\left[\frac{d^2}{dz^2} + k_z^{s2}(\omega^s)\right] E_x^s(\omega^s, k_x^s, z) = I(\omega^s, k_x^s, z),$$

where

$$I(\omega^s, k_x^s, z) = -\frac{4\pi i}{\omega^s \varepsilon(\omega^s)} \times \\ \times \left[k_z^{s2}(\omega^s) j_x^s(\omega^s, k_x^s, z) + ik_x^s \frac{dj_z^s(\omega^s, k_x^s, z)}{dz}\right] \qquad (12)$$

and $k_z^s(\omega^s) = \sqrt{\varepsilon(\omega^s)(\omega^s/c)^2 - k_x^{s2}}$ is the normal component of the wave vector in the medium for the scattered wave.

The scattered field in the vacuum $z < z_0$ is expressed in terms of $I(\omega^s, k_x^s, z)$:

$$E_x^s(\omega^s, k_x^s, z) = \frac{2\varepsilon(\omega^s)\omega^s \cos\theta^s/c}{k_z^s + \varepsilon(\omega^s)\omega^s \cos\theta^s/c} I_0 \times \\ \times \exp\left[-i(z - z_0)\omega^s \cos\theta^s/c\right],$$

$$E_z^s(\omega^s, k_x^s, z) = \frac{k^s \omega^s \cos\theta^s}{c k_z^{s2}} E_x^s(\omega^s, k_x^s, z),$$

where

$$I_0 = \frac{i}{2k_z^s} \int_{z_0}^{\infty} dz' \exp\left[ik_z^s(z' - z_0)\right] I(\omega^s, k_x^s, z') \qquad (13)$$

and θ^s is the propagation angle of scattered wave in the vacuum.

The energy flow from the surface of the sample is given by $|E_x^s(\omega_s, k_x^s, z < z_0)|^2$. Therefore, we have to calculate

$$\langle I^*(\omega^s, k_x^s, z) I(\omega^s, k_x^s, z')\rangle \qquad (14)$$

averaged quantum-mechanically and statistically, where according to Eqs. (12) and (11), we meet the Fourier transform of the correlation function

$$K_{jk,j'k'}(t, \mathbf{r}; t', \mathbf{r}') = \langle \mathcal{N}_{jk}^*(t, \mathbf{r}) \mathcal{N}_{j'k'}(t', \mathbf{r}')\rangle.$$

Because this correlator depends on the differences $t - t'$ and $x - x'$, we can expand it in the Fourier integral with

respect to these differences. Then, we have the Fourier transform $K_{jk,j'k'}(\omega, k_x, z, z')$, which can be expressed in terms of the generalized susceptibility according to the fluctuation–dissipation theorem:

$$K_{jk,j'k'}(\omega, k_x, z, z') = \\ = \frac{2}{1-e^{-\omega/T}} \mathrm{Im}\, \chi_{jk,j'k'}(\omega, k_x, z, z').$$

The generalized susceptibility $\chi_{jk,j'k'}(\omega, k_x, z, z')$ is involved in the response

$$\langle \mathcal{N}_{jk}(\omega, k_x, z)\rangle = \\ = -\int_{z_0}^{\infty} dz' \chi_{jk,j'k'}(\omega, k_x, z, z') U_{j'k'}(\omega, k_x, z') \quad (15)$$

to the force

$$U_{jk}(\omega = \omega^i - \omega^s, k_x = k_x^i - k_x^s, z) = \\ = A_j^s(\omega^s, k_x^s, z) A_k^i(\omega^i, k_x^i, z) \propto e^{iq_z z},$$

where $q_z = k_z^i + k_z^s$.

To calculate the generalized susceptibility $\chi_{jk,j'k'}(\omega, k_x, z, z')$, we write the equations for the averaged phonon $\mathbf{u}$ and plasmon $\mathbf{E}$ fields. In the right-hand side of the motion equation for the phonon field,

$$(\omega_{TO}^2 - \omega^2 - i\omega\Gamma) u_i(\omega, k_x, z) = \\ = \frac{Z}{\rho} E_i(\omega, k_x, z) - \frac{g_{ijk}^u}{\rho} U_{jk}(\omega, k_x, z), \quad (16)$$

the variation of Hamiltonian (9) with respect to the vibrations $\mathbf{u}$ gives an additional term to the force from the electric field; ρ is the density of the reduced mass and Z is the effective charge.

The equation for the plasmon field $\mathbf{E}$ can be obtained if this field is taken as a variable in Hamiltonian (9):

$$\nabla \cdot (\mathbf{E} + 4\pi \mathbf{P}) = 4\pi\rho. \quad (17)$$

The charge density ρ is connected to the current by Eq. (5). The polarization $\mathbf{P}$ includes the dipole moment $Z\mathbf{u}$, the contribution $\chi_\infty \mathbf{E}$ of the filled electron state, and the variational term $-\delta\mathcal{H}/\delta\mathbf{E}$:

$$P_i = Z u_i + \chi_\infty E_i - g_{ijk}^E U_{jk}.$$

Here, we can put u_i from Eq. (16). In Eq. (17), we obtain the term with $\varepsilon_\infty = 1 + 4\pi\chi_\infty$ and $g_{ijk}^E \to \tilde{g}_{ijk}^E$:

$$\tilde{g}_{ijk}^E = g_{ijk}^E + \frac{g_{ijk}^u Z}{\rho(\omega_{TO}^2 - \omega^2 - i\omega\Gamma)}. \quad (18)$$

Equation (17) can be substantially simplified in the case under consideration where the the wave vectors $\mathbf{k}^i$, $\mathbf{k}^s$, and consequently the momentum transfer $\mathbf{k} = \mathbf{k}^i - \mathbf{k}^s$ are determined by the frequency of the incident optical radiation, whereas the frequency transfer ω of the excited fields $\mathbf{E}$ and $\mathbf{u}$ is much less than the incident frequency, $\omega = \omega^i - \omega^s \ll \omega^i$. Therefore, we can neglect the retardation terms ω/c compared to k_x (so that $\kappa = k_x$) and introduce the potential, $\mathbf{E} = -\nabla\phi$. We obtain the following equation for the potential:

$$\left(\frac{d^2}{dz^2} - k_x^2 + 2k_x C \sum \delta(z - z_l)\right) \phi(\omega, k_x, z) = \\ = -\frac{4\pi}{\varepsilon(\omega)} \left(ik_x \tilde{g}_{xjk}^E + \tilde{g}_{zjk}^E \frac{d}{dz}\right) U_{jk}(\omega, k_x, z). \quad (19)$$

The solution of this equation is found by using the Green's function obeying the same Eq. (19) but with the $\delta(z - z')$ function in the right-hand side. As is very well known, the Green's function is expressed in terms of the solutions of the corresponding homogeneous equation. With $f_\pm(\omega, k_x, z)$ from Eq. (6), we write

$$G(z, z') = \frac{i}{2\kappa \sin(k_z d)\,\mathrm{sh}\,(\kappa d)} \times \\ \times \begin{cases} f_+(z) f_-(z'), & z > z', \\ f_-(z) f_+(z'), & z < z', \end{cases} \quad (20)$$

where the quasi-momentum $k_z = k_z(\omega^s, \kappa)$ has to be determined from dispersion relation (7) ignoring the retardation, $\kappa = k_x$.

According to the T_d symmetry of the GaAs lattice, the Raman tensors g_{ijk}^u and g_{ijk}^E have only two independent components, g_{xxx} and g_{xyz}, in the crystal axes. Let the scattered light be always polarized in the xz plane. We now consider two geometries. For the parallel scattering geometry (a), the incident light is considered to be polarized in the x direction, then the x-components of the exited phonon and plasmon fields can be active in the Raman scattering due to g_{xxx}. For the crossed geometry (b), the incident light is polarized in the y direction. Then, z-components of the exited fields are active and we take the terms with g_{xyz} into account. Thus, for the generalized susceptibility $\chi_{xx,xx}(\omega, k_x, z, z')$ defined by Eq. (15), we have

$$\chi_{xx,xx}(\omega, k_x, z, z') = \frac{g_{xxx}^{u2}/\rho}{\omega_{TO}^2 - \omega^2 - i\omega\Gamma} \delta(z - z') - \\ - \frac{4\pi k_x^2}{\varepsilon(\omega)} \tilde{g}_{xxx}^E G(z, z'). \quad (21)$$

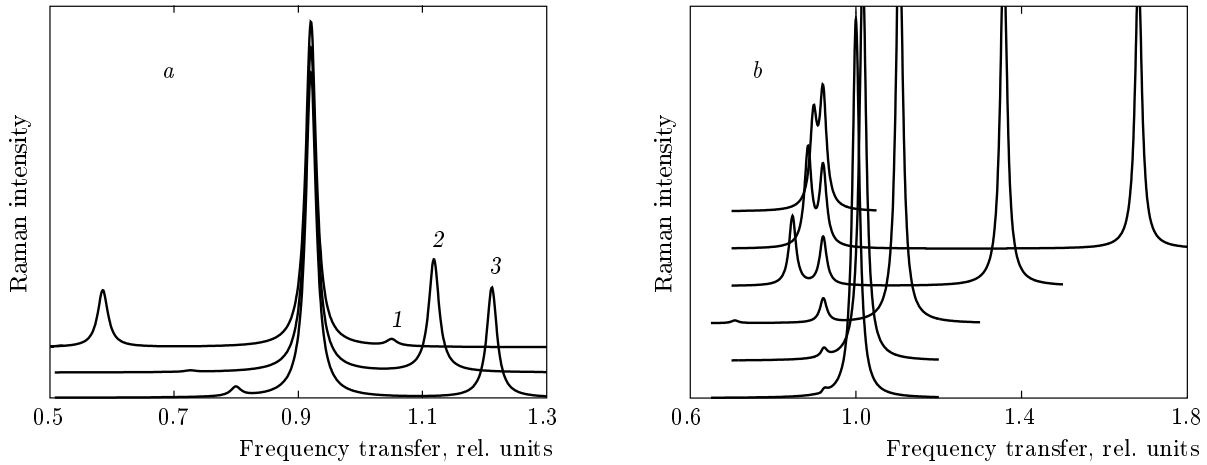

Fig. 7. Raman intensity versus the frequency transfer (in units ω_{LO}): (a) for three values of the carrier concentration ($n_e = 0.8 \cdot 10^{12}$ cm^{-1} (curve *1*), $n_e = 1.4 \cdot 10^{12}$ cm^{-1} (curve *2*), and $n_e = 2 \cdot 10^{12}$ cm^{-1} (curve *3*)) in the parallel-polarization geometry with the scattering direction making the angle of $\pi/4$ with the backscattering direction and (b) for the crossed polarization with the scattering angle varying from 0 (bottom) to $\pi/2$ (top) by the step of $\pi/10$ and the carrier concentration $n_e = 2 \cdot 10^{12}$ cm^{-2}. The values of the other parameters are the same as in Fig. 2

To obtain the Raman cross section, Eq. (14), we evaluate the integral

$$\int\limits_{z_0}^{\infty} dz\, dz' \exp[i(q_z z' - q_z^* z)]\, \mathrm{Im}\, \chi_{ij,ij}(k, \omega, z, z'),$$

where the asterisk denotes a complex conjugation. For the terms with $G(z, z')$, we obtain

$$\mathrm{Int} = \int\limits_{z_0}^{\infty} dz f_-(z) \int\limits_{z}^{\infty} dz' f_+(z') \exp[i(q_z z' - q_z^* z)] + \\ + \int\limits_{z_0}^{\infty} dz f_+(z) \int\limits_{z_0}^{z} dz' f_-(z') \exp[i(q_z z' - q_z^* z)],$$

where the first term is

$$\int\limits_{z_0}^{\infty} dz f_-(z) \int\limits_{z}^{\infty} dz' f_+(z') \exp[i(q_z z' - q_z^* z)] = \\ = \sum_{n,m=0}^{\infty} \exp[i(q_z - q_z^*)nd + i(k_z - q_z)md] \times \\ \times \int\limits_{z_0}^{z_0+d} dz\, f_-(z) \int\limits_{z}^{z+d} dz' f_+(z') \exp[i(q_z z' - q_z^* z)]. \quad (22)$$

The sum over the integer n can be extended to infinity, being then equal to $\delta/2d$, if the thickness of the sample is larger compared to the skin-depth δ of the incident or scattered waves. The sum over m reduces to a nonvanishing factor only under the Bragg condition $k_z - q_z = 2\pi n/d$, which expresses the momentum conservation law in the exciting processes of the phonon–plasmon coupled modes. In the macroscopic limit, when the wave length of the exited mode is large compared to the period d, only the main Bragg maximum ($n = 0$) is observed for each of the coupled modes. In this case, we can expand the matrix element in Eq. (22) in powers of $k_x d$ and $k_z d$.

Omitting the overall factors, we have the Raman intensity for the parallel geometry (a) in the form

$$\mathrm{Int}_{xx}(\omega, k_x) = \mathrm{Im} \left\{ \frac{g_{xxx}^{u2}/\rho}{\omega_{TO}^2 - \omega^2 - i\omega\Gamma} + \right. \\ \left. + \left(g_{xxx}^E + \frac{g_{xxx}^u Z/\rho}{\omega_{TO}^2 - \omega^2 - i\omega\Gamma} \right)^2 \frac{4\pi k_x^2}{(k_z^2 - q_z^2)\varepsilon(\omega)} \right\} \quad (23)$$

and for the crossed geometry (b),

$$\mathrm{Int}_{xy}(\omega, k_x) = \mathrm{Im} \left\{ \frac{g_{xyz}^{u2}/\rho}{\omega_{TO}^2 - \omega^2 - i\omega\Gamma} + \right. \\ \left. + \left(g_{xyz}^E + \frac{g_{xyz}^u Z/\rho}{\omega_{TO}^2 - \omega^2 - i\omega\Gamma} \right)^2 \frac{4\pi q_z^2}{(k_z^2 - q_z^2)\varepsilon(\omega)} \right\}. \quad (24)$$

The wave vector k_z of the coupled phonon–plasmon mode is determined by Eq. (7). For example, if the incidence is normal to the sample surface and θ is the scattering angle, then

$$k_x = \frac{\omega^i \sin\theta}{c}, \quad q_z = \frac{\omega^i}{c} \left[\sqrt{\varepsilon(\omega^i)} + \sqrt{\varepsilon(\omega^i) - \sin^2\theta} \right],$$

where we take into account that $\omega^i \approx \omega^s$.

In Eqs. (23) and (24), we dropped slowly varying factors depending on the parameters of the incident and scattered radiations, for instance, their dielectric constants as well as the temperature factor $1/[1+\exp(-\omega/T)]$. In numerical calculations, we used the relation between the vertices g^u and g^E known from experiments and given by the Faust–Henry constant

$$C_{FH} = g^u Z/g^E \rho \omega_{TO}^2 = -0.5.$$

The results of calculations are shown in Fig. 7.

We note that for the case of normal propagation of both incident and scattered radiation, $k_x = 0$, the second term in Eq. (23) vanishes, and the Raman peak at parallel polarizations (geometry a) is situated at the frequency ω_{TO}. The other peaks in Fig. 7*a* correspond to the excitations of the coupled phonon–plasmons. But for the crossed polarizations (geometry (b)) and $k_x \to 0$, the dispersion equation (7) with $C \to 0$ gives $k_z = ik_x$. Then, using Eq. (24) and the relation $\omega_{LO}^2 - \omega_{TO}^2 = 4\pi Z^2/\varepsilon_\infty \rho$ between the frequencies of the LO and TO phonons, we see that the peak occurs only at ω_{LO}, because the terms with poles at ω_{TO} are cancelled. This peak corresponds to a zero of dielectric constant $\varepsilon(\omega)$. At other scattering angles, a peak appears at ω_{TO} independently of the scattering angle. Two other peaks on each curves in Fig. 7*b* correspond to the excitation of the phonon–plasmons.

5. CONCLUSIONS

In this work, we investigated the infrared absorbtion and Raman scattering on the coupled phonon–plasmon modes with the help of a simple model of superlattices formed by thin conducting layers separated with insulating layers. This model admits a dispersion relation of an analytical form. Our results for the reflectance and the Raman spectra show that the observed picture can be drastically modified by means of the carrier concentration, the superlattice period, and the frequency.

One of the authors (L. A. F.) is grateful to J. Camassel for collaboration at GES (Montpellier, CNRS) and P. Fulde (Dresden, MPIPKS) for hospitality. The work was supported by the Russian Foundation for Basic Research (project № 04-02-17087).

REFERENCES

1. I. Yokota, J. Phys. Soc. Jpn. **16**, 2075 (1961); B. B. Varga, Phys. Rev. **137**, A1896 (1965); K. S. Singwi and M. P. Tosi, Phys. Rev. **147**, 658 (1966).

2. A. Mooradian and G. B. Wright, Phys. Rev. Lett. **16**, 999 (1966); A. Mooradian and A. L. McWhorter, Phys. Rev. Lett. **19**, 849 (1967).

3. E. L. Ivchenko and G. E. Pikus, *Superlattices and Other Heterostructures*, Vol. 110, Springer, Berlin (1997).

4. F. Stern, Phys. Rev. Lett. **18**, 546 (1967).

5. H. Sato and Y. Hori, Phys. Rev. B **39**, 10192 (1989).

6. F. M. Peeters, X. Wu, and J. T. Devreese, Phys. Rev. B **36**, 7518 (1987).

7. C. Faugeras, G. Martinez, A. Riedel, R. Hey, K. J. Friedland, and Yu. Bychkov, Phys. Rev. Lett. **92**, 107403 (2004); Yu. Bychkov, C. Faugeras, and G. Martinez, Phys. Rev. B **70**, 085306 (2004).

8. A. L. Fetter, Ann. Phys. **88**, 1 (1974).

9. S. Das Sarma and J. J. Quinn, Phys. Rev. B **25**, 7603 (1982); G. Qin, G. F. Giuliani, and J. J. Quinn, Phys. Rev. B **28**, 7603 (1982); A. C. Tselis and J. J. Quinn, Phys. Rev. B **28**, 2021 (1983); A. C. Tselis and J. J. Quinn, Phys. Rev. B **29**, 3318 (1984).

10. E. G. Mishchenko and A. V. Andreev, Phys. Rev. B **65**, 235310 (2002).

11. L. A. Falkovsky and E. G. Mishchenko, Pis'ma v Zh. Eksp. Teor. Fiz., **82**, 103 (2005).

12. W. Limmer, M. Glunk, S. Mascheck et al., Phys. Rev. B **66**, 205209 (2002).